Optimal Modulator with Loudspeaker Parameter Inclusion

Dahl, Nicolai Jerram; Iversen, Niels Elkjær; Knott, Arnold

Published in:
Proceedings of the 1^{43rd}Audio Engineering Convention Convention

Publication date:
2017

Document Version
Peer reviewed version

Audio Engineering Society

Convention Paper

Presented at the 143rd Convention
2017 October 18–21, New York, NY, USA

Optimal Modulator with Loudspeaker Parameter Inclusion

Nicolai J. Dahl[1], Niels E. Iversen[1], and Arnold Knott[1]

[1]*Technical University of Denmark*

Correspondence should be addressed to Nicolai Dahl (nicolai@jerram.dk)

ABSTRACT

Today, most class-D amplifier designs are able to deliver high efficiency and low distortion. However, the effect of parasitic components and speaker dynamics are not taken into account, resulting in a degradation of the performance. This paper proposes a new PWM modulator which is able to capture an arbitrary amount of dynamics through optimization based design methods. This makes it possible to include the parasitic components in the amplifier and the loudspeaker parameters in the design, thus creating a more linear response.

1 Introduction

Today class-D amplifiers are a common pick of choice when high efficiency and power are needed in an application. The high efficiency is achieved by using a switching power stage meaning the output is either fully on or fully off [1, 2]. This results in a reduction of the losses in the amplifier thus minimizing the power dissipation. The switching signal in the class-D amplifier is generated by the modulator. The audio signal enters the modulator which generates a pulse coded signal, which usually is Pulse Width Modulated (PWM). The modulated output is amplified and then sent through a 2nd order low-pass filter before leaving the amplifier. The low-pass filter ensures that the switching transients are attenuated leaving only the amplified audio signal.

Today, multiple modulator topologies exist which can be used with just as many different control strategies. Among the different topologies for modulators, and the control hereof, it seems to be the ones that incorporate the power stage, and sometimes also the output filter, that perform the best [3, 4, 5]. Class-D amplifiers with Total Harmonic Distortion (THD) as low as 0.0012% have been achieved proving that both low distortion and high efficiency can be obtained [4, 6].

A common limitation for today's class-D amplifiers is that the designs are based around obtaining a low THD on the output voltage of the amplifier. This results in the dynamics of the loudspeaker often being neglected in the design process and thus replaced by a purely ohmic resistance. This approach is not optimal since the loudspeaker introduces uncontrolled non-linear dynamics, thus increasing the THD with sereval orders of magnitude before the sound reaches the ears of the listener. [7, 8]. The design methods also tend to assume that the output filter is ideal, resulting in the effect of the parasitic components being neglected thus increasing the uncertainty of the design.

In this paper, a self-oscillating modulator topology for class-D amplifiers is proposed. This modulator is designed from an arbitrary sized state space model, enabling the inclusion of parasitic components as well as loudspeaker parameters directly in the design. This is achieved by generalizing the design problem by

applying optimization procedures to find satisfactory solutions. The result of this is the possibility to include feedback signals from the speaker directly back into the modulator which helps flatten the frequency response and reducing the non-linearities of the speaker.

2 State Space Modelling

A class-D amplifier is, like any switch mode power amplifier, a piecewise continuous system which can be modelled as a Linear Time Invariant (LTI) model using the state space average model [9]. This method has been widely used as it provides an internal model of the system, thus making it suitable for describing the small signal transfer properties of the system [9, 10]. In the model, each state of the system is modelled separately for every switching state the system can assume. The models are then averaged with a weight based on the duty cycle of a selected linearization point. The duty cycle is a measure for the percentage of time the switching output is high in a switching period. For a half-bridge class-D amplifier only two switching states on a single signal need to be considered. This makes the modelling of the amplifier so simple that it is often beneficial to model full-bridge class-D amplifiers as half-bridge by applying a filter transformation [11]. Equation 1 shows the two switching states of a half-bridge class-D amplifier.

$$V_{sw} = \begin{cases} V_{cc} & \forall\, dT_{sw} \\ -V_{cc} & \forall\, \bar{d}T_{sw} \end{cases} \tag{1}$$

Since audio is an AC signal, the linearization point will usually be selected to be in the center of the AC signal. For a class-D amplifier, this would result in the linearization point where the duty cycle is $d = 0.5$. This linearization point has the nice property of making the averaged state space model equivalent to the standard state space model. Equation 2 shows the state evolution of the standard state space description for a LTI system and Equation 3 shows the corresponding output.

$$\dot{x}(t) = Ax(t) + Bu(t) \tag{2}$$
$$y(t) = Cx(t) \tag{3}$$

When constructing the state space model, all the dominant internal states must be modelled. This makes the minimum order of the model to be at least equal to the order of the output filter of the amplifier. Naturally, it is desirable to include more dynamics to the model to get a better description of the amplifier. Besides modelling the amplifier, the model can be extended to also include loudspeaker parameters or a crossover network if desired. This will result in the possibility of linearizing the loudspeaker, hence reducing the harmonic distortion introduced by its non-linearities. One should keep in mind that all the states selected for the model must be measurable in some way if only an analog controller is desired. Equation 4 shows the states selected for this paper which are: The capacitor voltage, the speaker current and the inductor current. The capacitor voltage and inductor current are used to model the 2nd order output filter and are the most suitable choice as both states are easily measured. The speaker current is used to model the inductance of the voice coil in the loudspeaker. This limited amount of states are selected to avoid the need for a digital controller. Figure 1 shows a diagram of the modelled circuit.

$$x(t) = \begin{bmatrix} I_{ind} \\ I_{spk} \\ V_c \end{bmatrix} \tag{4}$$

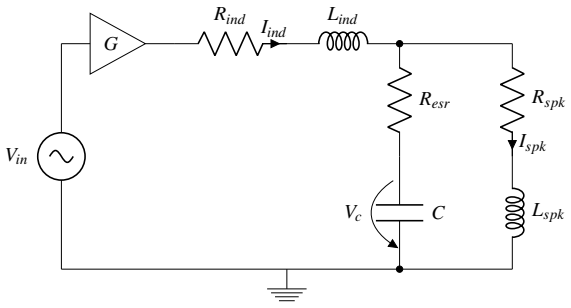

Fig. 1: The circuit modelled in the state space model. Multiple parasitics are considered

Here G is the open-loop gain of the comparator and will usually be in the tens of thousands. The output of G, however, is limited by the supply voltage V_{cc} placing a bound on the signal. Writing up the circuit equations and doing the linearization, the system matrix A and the input matrix B is found (Eq. 5).

$$A = \begin{bmatrix} -\frac{R_{ind}+R_{esr}}{L_{ind}} & \frac{R_{esr}}{L_{ind}} & -\frac{1}{L_{ind}} \\ \frac{1}{L_{spk}} & -\frac{R_{spk}+R_{esr}}{L_{spk}} & \frac{1}{L_{spk}} \\ \frac{1}{C} & -\frac{1}{C} & 0 \end{bmatrix} \quad B = \begin{bmatrix} \frac{G}{L_{ind}} \\ 0 \\ 0 \end{bmatrix} \tag{5}$$

The output matrix C is usually selected to be the last state the signal propagates through. In this case, it is the speaker current I_{spk} which is also evident from Figure 1. Equation 6 shows the output matrix.

$$C = \begin{bmatrix} 0 & 1 & 0 \end{bmatrix} \tag{6}$$

3 System Design

Using the state space description of the class-D amplifier, the feedback for both the modulator and control can be calculated.

3.1 Self-Oscillating Modulator

Self-oscillating modulators are a family of modulators where the generation of the carrier waveform, used for the oscillation, is embedded into the modulator. These modulators have the benefits of lower EMC and increased system bandwidth compared to fixed frequency modulators [12]. The self-oscillation is achieved by feeding back a filtered version of the modulators own output to itself while preventing the modulator from reaching a stable state. The stable state is prevented by either using a hysteresis window [13, 3] or introducing 180° of phase-shift in the feedback signal [6]. The filter can be realized in multiple ways where some common methods are: to use an RC-network directly from the output of the modulator [13] or to use the ripple current I_Δ through the output filter inductor L_{ind} [5]. The last mentioned method will be used here to create a hysteresis based modulator.

When designing a self-oscillating modulator, it is desired to control two key parameters: The idle switching frequency f_{idle} of the modulator and the gain through the modulator. These parameters can be controlled through the feedback gains to the modulator allowing for the two parameters to be designed independently. Figure 2 shows the modulator with the feedback gains k_1 and k_2 coming from the inductor current and capacitor voltage as specified in Figure 1. These two feedback signals form the carrier signal $V_{car}(t)$ which is used for driving the modulator. The size of the hysteresis window V_{hys} is specified by the two resistors R_1 and R_2 by conventional means.

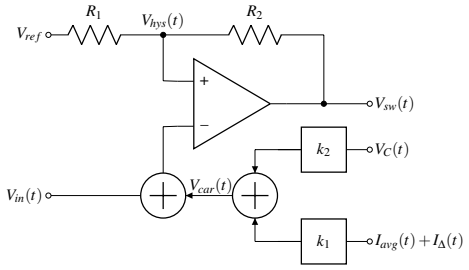

Fig. 2: Modulator with the feedback signals for the carrier waveform generation

The idle switching frequency is the switching frequency when no signal is applied to the amplifier. This simplifies the design as the output voltage will be approximately zero resulting in only the inductor current needing consideration. The current in the inductor is the first state in the state space description, making it easy to isolate. Thus the evolution of the state can be easily determined. Equation 7 shows the system matrix A where the inductor current state has been isolated in the upper left corner (A_{11}).

$$A = \left[\begin{array}{c|cc} -\frac{R_{ind}+R_{esr}}{L_{ind}} & \frac{R_{esr}}{L_{ind}} & -\frac{1}{L_{ind}} \\ \hline \frac{1}{L_{spk}} & -\frac{R_{spk}+R_{esr}}{L_{spk}} & \frac{1}{L_{spk}} \\ \frac{1}{C} & -\frac{1}{C} & 0 \end{array}\right] \tag{7}$$

With the inductor current state isolated, the evolution of the state can easily be found through Equation 8.

$$I_{ind}(t) = \int_0^\infty \mathrm{e}^{A_{11}(t-\tau)} B u(t)\,\mathrm{d}\tau \tag{8}$$

$$= -\frac{V_{cc}\left(\mathrm{e}^{-\frac{R_{ind}+R_{esr}}{L_{ind}}t} - 1\right)}{R_{ind}+R_{esr}} \tag{9}$$

Equation 9 shows the resulting exponential function describing the state evolution of the inductor current. Here the gain, G, from the input matrix B is in its saturated state, hence being the supply voltage V_{cc}. Multiplying with the feedback gain k_1 and isolating the time

t, the idle frequency can be determined as the time it takes to charge from the lower threshold of the hysteresis window to the upper threshold of the hysteresis window. Equation 10 shows the function for the idle switching frequency.

$$f_{idle} = \frac{1}{(t_{high} - t_{low}) \cdot 2} = -\frac{R_{ind} + R_{esr}}{2L_{ind} \ln\left(\frac{4k_1 V_{cc}}{2k_1 V_{cc} + V_{hys}(R_{ind}+R_{esr})} - 1\right)} \tag{10}$$

Since it is the feedback gain k_1 that needs to be determined, k_1 in Equation 10 is isolated. Equation 11 shows the equation to determine k_1 based on a desired switching frequency, hysteresis window size, inductor size and parasitics.

$$k_1 = \frac{V_{hys}(R_{ind} + R_{esr}) \coth\left(\frac{R_{ind}+R_{esr}}{4L_{ind} f_{idle}}\right)}{2V_{cc}} \tag{11}$$

The feedback signal from the inductor through k_1 will provide a voltage measurement of the scaled ripple current which is used as the carrier voltage for the modulator. However, the average current, I_{avg}, due to the audio signal is also contained within the feedback signal. This is undesirable as only the carrier voltage is needed. To avoid the average current, another feedback path from the capacitor voltage is included. The capacitor voltage will at low frequencies be in phase and proportional with the current in the inductor. Thus the carrier voltage can be isolated by subtracting the scaled capacitor voltage from the scaled inductor current. Equation 12 shows how the feedback gain k_2 can be found for the capacitor voltage. Here the proportionality between the current through the amplifier and the voltage across the capacitor when the system is saturated is used.

$$k_2 = -k_1 \frac{I_{sat}}{V_{sat}} \tag{12}$$

The inclusion of an additional feedback path also has the advantage of helping to suppress possible carrier distortion since an offset due to distortion would create a change in the capacitor voltage which would be feedback and thus suppressed. With the two modulator feedback gains designed, a closed-loop description can be obtained for use with the controller design. Equation 13 shows the closed-loop description.

$$A_{mod} = A - BK_{mod} \quad K_{mod} = \begin{bmatrix} k_1 & 0 & k_2 \end{bmatrix} \tag{13}$$

3.2 Linear Quadratic Regulator

The Linear Quadratic Regulator (LQR) is a special type of full state feedback controllers where the control problem is solved as an optimization problem [14]. This allows for an optimal selection of feedback gains and thus an optimal closed-loop response of the system. The LQ-controller is significantly different from the commonly used PID-controller in the fact that it uses feedback from each state in the system. This makes it possible for the controller to act quicker to possible changes, but more importantly, it makes it possible to change the dynamics of the system without increasing the order hereof [15, 14]. This enables the controller to flatten the response in the audio band through the entire system, thus also improving the audio properties of the loudspeaker. It is also common to see a significant reduction of the noise propagating through the system, resulting in an increase in the signal to noise ratio and the power supply rejection ratio [11]. This, however, comes with the drawback that complete state knowledge must be acquired, resulting in the potential need of an observer in cases where the states cannot be measured.

When designing a LQ-controller, a cost function needs to be made. This cost function specifies the control objective which the controller will need to minimize. Equation 14 shows a scalar cost function designed for amplifiers.

$$J(u) = \lim_{t\to\infty} \int_0^t \left(u(t) - \frac{y(t)}{G_{cl}}\right)^2 \mathrm{dt} \tag{14}$$

Inspecting Equation 14 it can be seen that the design goal is to minimize the difference between the control signal $u(t)$ and the output of the system $y(t)$ which is amplified by the closed-loop system gain G_{cl}. This will result in the controller trying to maintain the gain G_{cl} while minimizing any resonances in the system as these will increase the cost. To find the optimal solution to the cost function, the control problem needs

to be reformulated as a Ricatti equation from where an optimal solution K_∞ is obtained [14].

In cases where high order state space models are used to model the loudspeaker, see [16], it will not be possible to measure every single state, thus an observer must be implemented to estimate the remaining states. Observers are usually implemented on microcontrollers for practical reasons meaning that an analog-digital combined control loop needs to be made. Here all the measurable states will have their own analog feedback and only the estimated states will have a digital feedback.

3.3 System Merging

The feedback path of the modulator feedback and the LQR feedback both require the inductor current and the capacitor voltage to function properly. For the inductor current, the modulator uses the ripple current I_Δ to create the carrier voltage $V_{car}(t)$ used for the self-oscillation. On the other hand, the LQR is only designed to work with linear continuous signals thus the performance is degraded by the ripple current being superimposed on the control signal. This seems to impose two conflicting demands to the property of the measured inductor current. To clarify the situation, Figure 3 shows the modulator with the LQR feedback entering from the left side along with the audio input forming the control signal $u(t)$, and the modulator feedback entering from the right side creating the carrier voltage $V_{car}(t)$. Only the relevant LQR feedback signals are shown.

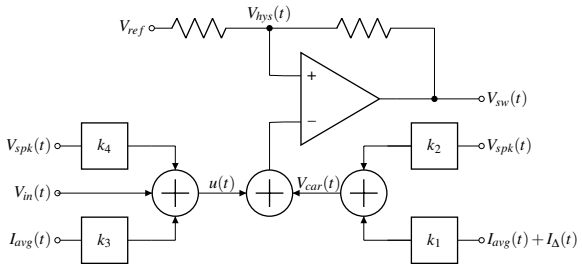

Fig. 3: Modulator with the feedback from the LQ-controller and the modulator gains

A classical solution to accommodate these conflicting demands of the inductor current would be to introduce a low-pass filter for the signal going to the LQR as this would attenuate the ripple current. However, this would increase the complexity of the system and it would be hard to obtain a desirable attenuation without introducing a phase shift in the audio band, potentially making the control less efficient or unstable. Due to these drawbacks, a novel solution is proposed which is based around merging the feedback structure of the LQR and the modulator. Looking at Figure 3, the equation for describing the signal on the negative input terminal of the comparator V_{in-} can be constructed. Equation 15 shows this equation with the time dependency omitted.

$$\begin{aligned} V_{in-} &= V_{car} + u \\ &= V_{spk}(k_2+k_4) + I_{avg}(k_1+k_3) + I_\Delta k_1 + V_{in} \end{aligned} \tag{15}$$

From Equation 15 it is evident that it is possible to add the gains from the same measurement to create a new gain with the same properties as the individual gains had. Unfortunately, by doing this the inductor ripple current becomes isolated which is just as problematic to realize as it was the other way around with the average inductor current. However, if it turns out that the LQR procedure always will set k_3 close to zero, a possibility for further reduction is created. Equation 16 shows the case where k_3 is approaching zero.

$$\lim_{k_3 \to 0} V_{in-} = V_{spk}(k_2+k_4) + (I_{avg}+I_\Delta)k_1 + V_{in} \tag{16}$$

Equation 16 clearly shows that if the assumption about k_3 is correct, the conflicting goals of the inductor current can be eliminated and a full integration of the linear quadratic regulator into the amplifier can be obtained. This would be very beneficial as it would allow for a less complex design and a simple method to include potential speaker measurements for regulation directly into the class-D amplifier. Further, the integration of the LQR also removes the constraints of the control signal, making it possible to design the controller without worrying about potential clipping of the audio signal. In short, an Optimal Modulator with Embedded Control (OMEC) could be realized. To validate the assumption about k_3, the cost function of the LQR and the modulator design method needs to be reviewed. The cost function (Eq. 14) focusses on obtaining a specific gain through the system while reducing the resonances in

the system. Thus, if the feedback gain for the modulator k_1 ensures well damped poles for the 2nd order low-pass filter, the LQR design routine will generate a small k_3 as the inductor current state will not be important to achieve the design goal. To see if k_1 results in a sufficient damping of the 2nd order low-pass filter, the filter is written in its simplest form where all the parasitics are ignored and the gain k_1 included. Equation 17 shows the transfer function of the filter and equation 18 shows the resulting damping factor ζ.

$$H(s) = \frac{\omega_c^2}{\omega_c^2\left(1+\frac{Gk_1}{R_{spk}}\right)+s\left(\frac{1}{R_{spk}C}+\frac{Gk_1}{L_{ind}}\right)+s^2} \quad (17)$$

$$\zeta = \frac{\frac{1}{R_{spk}C}+\frac{Gk_1}{L_{ind}}}{2\omega_c} \quad (18)$$

Since G is the open-loop gain of the comparator, it is evident from equation 18 that even extremely small positive values of k_1 will result in an overdamped filter, thus it can be concluded in general that k_3 will be close to zero, resulting in Equation 16 being valid.

By injecting the LQR control loop directly into the modulator, as done with the proposed method, the size of the control signal will not induce any limitations for additional control loops. This results in an overall improvement in the performance regarding linearity, noise, and power supply rejection, without imposing any limitations on the remaining system.

4 Example System

To evaluate the performance of the OMEC class-D amplifier, a switching model for simulation has been constructed in Simulink. Table 1 shows a table with the specifications of the amplifier used in the simulation. Equation 19 and 20 show the corresponding system and input matrix. These matrices have the same structure as the previously shown, hence both the capacitor's ESR and the inductance of the loudspeaker's voice coil are included. Please note that while the first element in B has an exact description, it can in practice be selected to be any large number because of the gain of the comparator.

Cutoff Frq (f_c)	35	kHz
Damping factor (ζ)	0.1	
Idle Switch Frq (f_{sw})	500	kHz
Rail Voltage (V_{cc})	$\pm$40	V
Maximum Power (P_{max})	200	Wrms
Speaker resistance (R_{spk})	4	Ω
Speaker inductance (R_{ind})	20	μH

Table 1: Class-D Amplifier Specifications

$$A = \begin{bmatrix} -6185 & 2748.9 & -1.3744\cdot 10^5 \\ 1000 & -2.01\cdot 10^5 & 50000 \\ 1.7593\cdot 10^5 & -1.7593\cdot 10^5 & 0 \end{bmatrix} \quad (19)$$

$$B = \begin{bmatrix} 6.8722\cdot 10^{12} \\ 0 \\ 0 \end{bmatrix} \quad (20)$$

First the modulator feedback gains K_{mod} are found using Equation 11 and 12. The resulting closed-loop description is then used to find the controller feedback gains K_∞ using the LQR method. Equation 21 shows the combined feedback gains for the class-D amplifier. The order of the gains corresponds to the order of the state vector (Eq. 4).

$$K = K_{mod} + K_\infty = \begin{bmatrix} 0.090946 & -0.12381 & 0.11691 \end{bmatrix} \quad (21)$$

The controller feedback gains have been selected such that a sufficient bandwidth of the closed-loop system is achieved. This, however, results in a low gain of the system. A frequency analysis is carried out to evaluate the system's performance. Figure 4 shows the bode plot of the system before and after the LQR control is applied. Here it is seen that the achieved bandwidth of the system after the LQR control is applied is 22.2 kHz and thus sufficient for audio applications. This bandwidth has come with the cost of a lower gain through the system compared to without the LQR. The gain is only 7.6 dB equivalent to a times 2.4 amplification from input to I_{spk}. This equals a voltage amplification of 19.7 dB or a 9.6 times amplification.

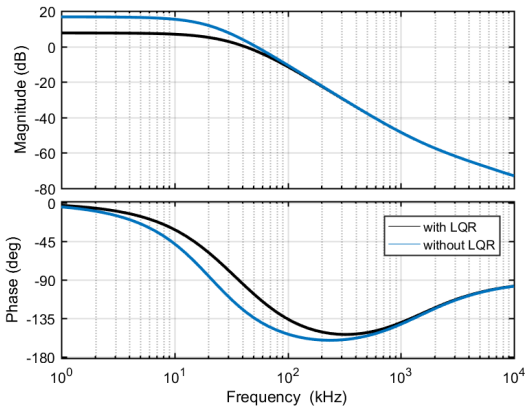

Fig. 4: Calculated frequency response of the closed-loop system from input to I_{spk}

The reason why it is hard to obtain better system performance than what has been found is that the output is chosen to be the current through the voice coil. This introduces additional dynamics to the system, thus slowing down the response. This also shows that a high bandwidth for the speaker voltage does not necessarily imply that a sufficient bandwidth is achieved in the speaker. To accommodate this, an increase of the cutoff frequency of the output filter and the switch frequency should be considered.

5 Results

Two simulations are conducted using the switching model. The first simulation is with zero input on the amplifier to verify that the idle switching frequency is as expected. Figure 5 shows the simulated carrier waveform when no input is applied. Measuring the time period shows that the idle switching frequency is exactly 500 kHz but in practice some deviation due to component tolerances is to be expected. Simulations also show that the response of the switching frequency to the input voltage have the known behaviours of hysteresis based self-oscillating modulators, meaning that the switching frequency will decrease as the amplitude of the input is increased [13, 12]. Figure 6 shows the second simulation. Here the system is given an input signal resulting in the amplifier delivering 50% of its maximum output (Fig. 6a) and 95% of its maximum output power (Fig. 6b). Both simulations are compared with the linearized model. The input signal is a sine wave with a frequency of 6.6 kHz which is the highest possible frequency before the third harmonic falls out of the audio band.

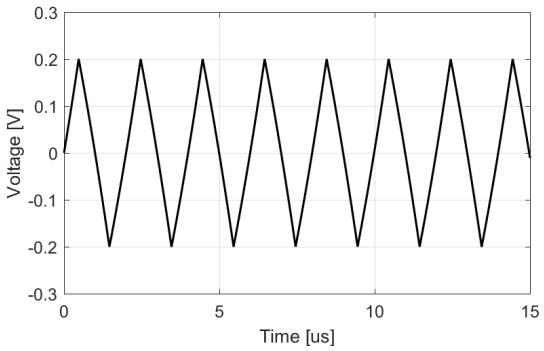

Fig. 5: Simulated carrier signal at 500 kHz with no input applied

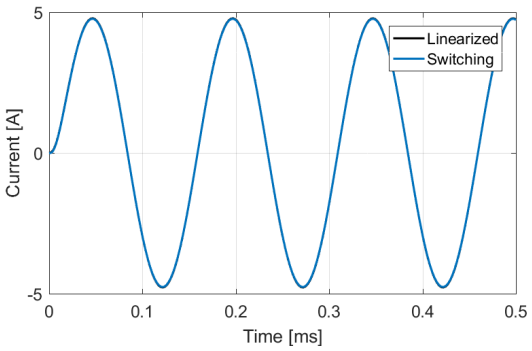

(a) Sinusoid at 50% output power. Hardly any distortion on the waveform

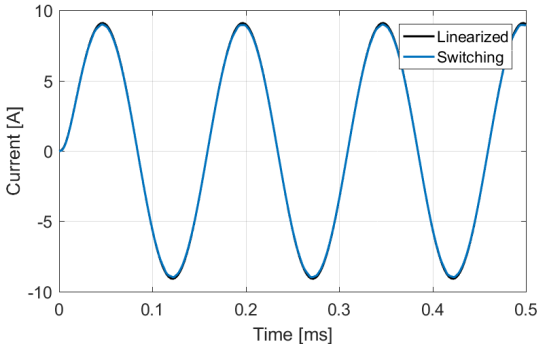

(b) Sinusoid at 95% output power. Distortion is just visible at the peaks

Fig. 6: Simulated sinusoid with a frequency of 6.66 kHz at 50% and 95% of total output power.

From Figure 6b it is seen that the modulator introduces some harmonic distortion when the system is close to clipping. To get a better idea of the total harmonic distortion (THD) a 10 round Monte Carlo simulation at 6.6 kHz with different amplitudes are conducted and the resulting THD+N averaged. Figure 7 shows the THD+N versus the output power of the amplifier. Two Gaussian white noise sources are included for these simulations to get more realistic results. The first noise source simulates input noise and has the distribution $N(0, 10^{-9})$. The second noise source simulates noise from the power supply and has the distribution $N(0, 0.01)$.

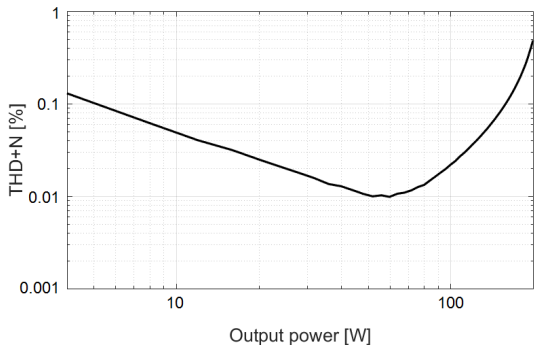

Fig. 7: Simulated THD+N from 4 W to 200 W output at 6.6 kHz

From Figure 7 it is seen that this specific OMEC modulator in theory is able to deliver harmonic distortion lower than 0.01% and no higher than 0.48%. It is possible to further reduce the THD by adding a global feedback loop around the system in the form of a PID or a $\mathscr{H}_2$ loop [15].

6 Summary

In this paper, a method for integrating a LQR control loop into a class-D amplifier has been presented. Methods for designing the feedback gains for the modulator and linear quadratic controller from state space models have been shown. By merging the feedback gains for the controller and the modulator, a simpler design was achieved while the performance of both feedback loops were preserved. The merge of the loops also resulted in the removal of constraints in the design process of the control loop and made it possible to include speaker parameters into the amplifier. Hereby, all the advantages of the control loop was retained e.g. better linearity, power supply rejection, and noise reduction, while the disadvantages was avoided. To verify the theory, simulations were made on a stochastic switching system model. These simulations showed that the properties of the class-D amplifier were preserved, thus agreeing with the theory. Lastly, theoretical THD+N measurements were made which showed that the simulated amplifier in average had THD+N lower than 0.01% and would never exceed 0.48%.

References

[1] Nielsen, K., "Audio power amplifier techniques with energy efficient power conversion," *Technical University of Denmark, Ph. D. Thesis April*, 1998.

[2] Duraij, M., Iversen, N. E., Petersen, L. P., and Boström, P., "Self-oscillating 150 W switch-mode amplifier equipped with eGaN-FETs," in *Audio Engineering Society Convention 139*, Audio Engineering Society, 2015.

[3] Poulsen, S. and Andersen, M. A., "Simple PWM modulator topology with excellent dynamic behavior," in *Applied Power Electronics Conference and Exposition, 2004. APEC'04. Nineteenth Annual IEEE*, volume 1, pp. 486–492, IEEE, 2004.

[4] Lu, J. and Gharpurey, R., "A self oscillating class D audio amplifier with 0.0012% THD+ N and 116.5 dB dynamic range," in *Custom Integrated Circuits Conference (CICC), 2010 IEEE*, pp. 1–4, IEEE, 2010.

[5] Poulsen, S. and Andersen, M. A. E., "Self oscillating PWM modulators, a topological comparision," in *Power Modulator Symposium, 2004 and 2004 High-Voltage Workshop. Conference Record of the Twenty-Sixth International*, pp. 403–407, IEEE, 2004.

[6] Putzeys, B., "Simple self-oscillating class D amplifier with full output filter control," in *Audio Engineering Society Convention 118*, Audio Engineering Society, 2005.

[7] Klippel, W., "Tutorial: Loudspeaker nonlinearities—Causes, parameters, symptoms," *Journal of the Audio Engineering Society*, 54(10), pp. 907–939, 2006.

[8] Bjerregaard, R., Madsen, A. N., Schneider, H., Agerkvist, F. T., and Andersen, M. A., "Accelerometer Based Motional Feedback Integrated in a 2 3/4" Loudspeaker," in *Audio Engineering Society Convention 140*, Audio Engineering Society, 2016.

[9] Polivka, W., Chetty, P., and Middlebrook, R., "State-space average modelling of converters with parasitics and storage-time modulation," in *Power Electronics Specialists Conference, 1980. PESC. IEEE*, pp. 119–143, IEEE, 1980.

[10] Nwosu, C. and Eng, M., "State-space averaged modeling of a nonideal boost converter," *The pacific journal of science and Technology*, 2(9), pp. 1–7, 2008.

[11] Dahl, N. J., Iversen, N. E., and Knott, A., "Optimal Control of a High Frequency Class-D Amplifier," Unpublished, 2017.

[12] Nielsen, D., Knott, A., Pfaffinger, G., and Andersen, M. A., "Investigation of switching frequency variations and EMI properties in self-oscillating class D amplifiers," in *Audio Engineering Society Convention 127*, Audio Engineering Society, 2009.

[13] Dahl, N., Iversen, N. E., Knott, A., and Andersen, M. A., "Comparison of Simple Self-Oscillating PWM Modulators," in *Audio Engineering Society Convention 140*, Audio Engineering Society, 2016.

[14] Hendricks, E., Jannerup, O., and Sørensen, P. H., *Linear systems control: deterministic and stochastic methods*, Springer Science & Business Media, 2008.

[15] Skogestad, S. and Postlethwaite, I., *Multivariable feedback control: analysis and design*, volume 2, Wiley New York, 2007.

[16] Madsen, F. S., Thorsen, S., Iversen, N. E., and Knott, A., "Model for Evaluation of Power Consumption of Vented Box Loudspeakers," in *Audio Engineering Society Convention 142*, Audio Engineering Society, 2017.